

The breakdown flash of Silicon Avalanche Photodiodes – backdoor for eavesdropper attacks?

Christian Kurtsiefer¹, Patrick Zarda², Sonja Mayer¹, and Harald Weinfurter^{1,2}

¹*Sektion Physik, Ludwig-Maximilians-Universität, D-80799 München, Germany*

²*Max-Planck-Institut für Quantenoptik, D-85748 Garching, Germany*

January 15, 2001

submitted to J. Mod. Opt.

Abstract

Silicon avalanche photodiodes are the most sensitive photodetectors in the visible to near infrared region. However, when they are used for single photon detection in a Geiger mode, they are known to emit light on the controlled breakdown used to detect a photoelectron. This fluorescence light might have serious impacts on experimental applications like quantum cryptography or single-particle spectroscopy. We characterized the fluorescence behaviour of silicon avalanche photodiodes in the experimentally simple passive quenching configuration and discuss implications for their use in quantum cryptography systems.

1 Introduction

For a long time, silicon avalanche photodiodes (APD) have been used for single photon detection in the near-infrared region[1, 2] because of their high quantum efficiency and low dark count rate. These properties are particularly important for quantum cryptography[3, 4, 5, 6], where a huge yield of secure bits and a low signal/noise ratio is crucial.

To obtain a single photon counting behaviour, the avalanche diode is operated in an all-or-nothing counting mode similar to the way Geiger detectors are used in nuclear physics for particle counting. In this so-called Geiger mode, the diode is reversely biased above the breakdown voltage such that a single photoelectron can generate a self-sustaining discharge. The discharge current is used as an indicator for the generation of a photoelectron and thus of an absorbed photon. Thereby, a timing accuracy better than 60 ps has been achieved[7].

It has been observed previously that the avalanche of charge carriers is accompanied by photon emission[8]. Although this light emission is not very strong, in several single photon counting applications it may have serious impacts on the experiment. In quantum cryptography, for example, such a light emission might enable an external observer to gain information of a photo detection event on the receiver side, opening a possible eavesdropping back door to an otherwise secure communication channel. Another experimental situation in which this photoemission has to be considered are photon correlation measurements, as they are performed in single atom or molecule spectroscopy. In a typical Hanbury-Brown–Twiss configuration, two photodetectors are looking onto a faint light source, and one has to ensure that light emitted in the breakdown flash of one photodiode is not causing artificial photo events in the second photodetector due to residual crosstalk between the two photodetectors[9, 10, 11]. It is therefore important to know the photoemission characteristics of that breakdown photoemission to avoid crosstalk with the light

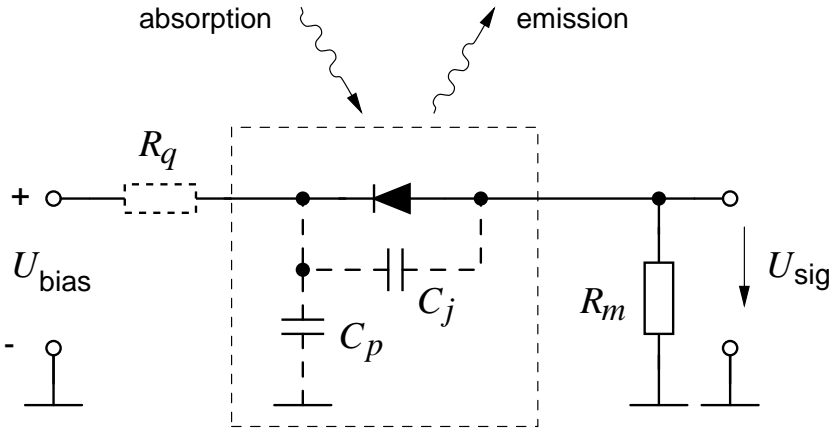


Figure 1: Operation of the APD in passive quenching mode. The diode (with a junction capacity C_j and a parasitic capacity C_p) is reverse biased via a high impedance quenching network R_q above the breakdown voltage. At diode breakdown, the parasitic capacity C_p discharges through the load resistance R_m , causing a voltage peak indicating the breakdown.

to be detected. In this paper, we describe our investigation of the temporal and spectral distribution as well as the absolute amount of light emitted during a detection event.

2 Photodiode operation

A photodetection process is initiated by a photoelectron created after absorption of a photon in a reverse-biased *pn*-junction. This electron is accelerated into a highly doped region where an avalanche of charge carriers is triggered. In single photon counting mode, the bias voltage exceeds the breakdown voltage of the diode, meaning that once an avalanche has been triggered, it is self-sustaining as long as the external voltage exceeds the breakdown threshold. To avoid the thermal damage of the diode and to bring it back into a state ready for a subsequent photoelectron detection, the avalanche has to be quenched. This is done by lowering the reverse bias voltage across the diode for a certain time. After allowing all charge carriers to recombine and thus bringing the diode into an insulating state again, a full photodetection cycle is finished and the diode is ready for the next event.

The usual configurations for that procedure are referred to passive and active quenching[12]. In passive quenching, the diode is reverse-biased via a low-current network (e.g. a large resistor R_q) such that the discharge current triggered by a photoelectron avalanche causes a voltage drop, reducing the voltage across the diode below the breakdown voltage (see figure 1). Then, the junction capacity C_j has to be recharged again to the full reverse bias voltage. With usual passive quenching configurations, a recharge time on the order of a microsecond is achieved. To obtain a faster recharge and thereby a shorter dead time, active quenching techniques have to be used[7]. Yet, the discharge current and thus the breakdown flash should not depend on the quenching configuration.

In our experiments, we used an APD with an integrated two stage thermoelectric cooler, type C30902-SDTC from Perkin-Elmer. The diodes have a circular active area of 0.5 mm diameter, and are accessible through a transparent window. They are mounted in modules together with a high voltage supply, a discriminator to generate standard NIM pulses and a temperature controller for the peltier element[13]. We use a current limiting network instead of a quenching resistor, a measurement resistor of $R_m = 100 \Omega$ and a reverse bias voltage of $U_{\text{bias}} = 215 \text{ V}$ at a temperature of -25°C , which is approximately 20 V above the breakdown of the APD. According to the manufacturer, the diodes are supposed

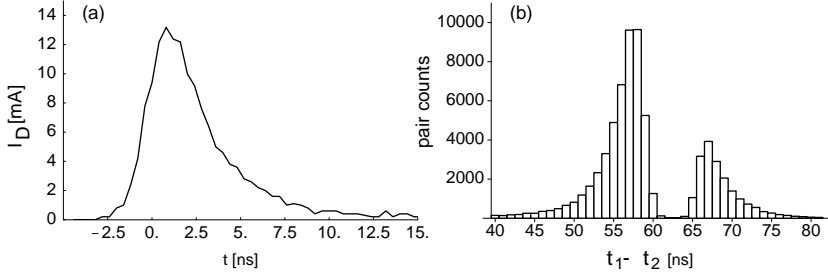


Figure 2: (a) Discharge current $I_D(T)$ of the avalanche photodiode during a breakdown cycle. (b) Histogram of coincidence events of both photodetectors. The left peak corresponds to photons emitted by diode 1 seen by diode 2. Both peaks have an exponential decay with a time constant of 2.9 ns. The asymmetry is due to the different magnification of the two diodes looking at each other. The shape of each peak resembles very much the discharge current behaviour.

to show a single photon detection efficiency of up to 55% at a wavelength of 800 nm[14], depending on operating conditions.

The discharge current $I_D(t)$ we measured under these conditions is shown in figure 2a. It reflects an exponential decay, convoluted with a Gaussian distribution. From this measurement, we obtain a total charge of

$$Q_D = \int T_D(t) dt = 64 \text{ pC}$$

released during a diode breakdown. From that value, we deduce a parasitic capacity C_p of

$$C_p = Q_D / 20 \text{ V} = 3.2 \text{ pF} ,$$

assuming that during breakdown, most of the current through R_m is supplied by C_p , and not by the biasing network.

3 Absolute photoemission rate

To determine the amount of light emitted during a breakdown cycle, we used an optical arrangement sketched in figure 3. The active area of an APD module D_1 is imaged with a lens $f = 50$ mm onto a second APD, D_2 , with a demagnification of 2 (corresponding to distances of $g = 150$ mm and $b = 75$ mm, respectively). This ensured that light emitted from all parts of the active area of diode D_1 could reach the active area of D_2 even for imperfect alignment. To define the solid angle of light collected from diode D_1 , we used an aperture A with a diameter of 3 mm (and 5 mm in a second experiment) at a distance of $d = 123$ mm from the diode. The corresponding solid angles are $\Omega_3 = 4.67 \cdot 10^{-4}$ sr and $\Omega_5 = 1.3 \cdot 10^{-3}$ sr, respectively.

The NIM pulses were sent both to PC-card based counters, and for timing analysis to a digital oscilloscope (LeCroy LC574A). Using a pair trigger feature together with an auxiliary delay line of 63 ns, we collected coincidence events of the two detectors and histogrammed their time differences $t_1 - t_2$ in an interval of -40 ns to +60 ns with a resolution of a few 100 ps.

To measure only the light emitted by the diode D_1 , we lowered the ambient light such that D_1 registered a count rate of $r_1 = 2634$ cps. This is only moderately larger than the dark count rate (approximately 500 cps) and ensures that scattering of external light to the second diode D_2 is minimal. With the optical path open to the second diode and an aperture diameter of 3 mm, we observe a count rate from diode D_2 of $r_2 = 731$ cps. Finally, only

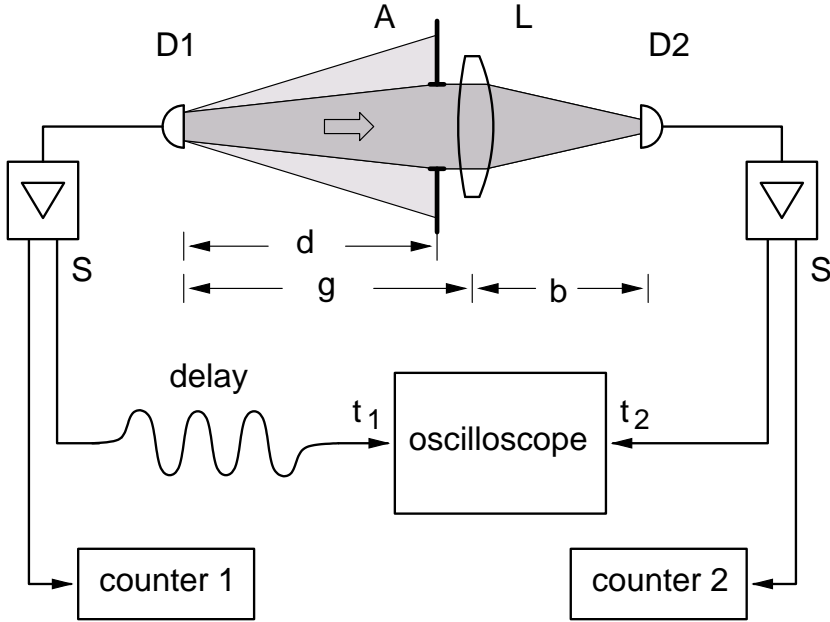


Figure 3: Setup to determine the integral fluorescence light. The active area of photodiode D_1 under investigation is imaged through a lens L onto a second photodiode D_2 , with an aperture A defining the solid angle seen of diode D_1 . Both diodes are operating in passive quenching Geiger mode. Their breakdown current is amplified, discriminated and sent to counters and an oscilloscope to investigate coincident events (The signal of D_1 is delayed by 63 ns).

pair events are selected which ensures that only the properties of the breakdown flash were analysed.

A histogram of time differences for double photo events is shown in figure 2b. One can clearly recognize two peaks, the left one ($t_1 - t_2 < 60$ ns) corresponding to photo events registered in detector D_2 after a discharge of detector D_1 , and the right one corresponding to the reverse process. The asymmetry in the amplitudes of the two peaks can be explained by the asymmetry in the imaging optics, as the aperture is not located exactly at the lens position, and/or by a difference in the amount light produced by the two diodes. Each peak shows a rise time between 1 and 2 ns, and an exponential decay, probably following the discharge current of the diode. The distribution $h(\Delta t)$ of each peak of time differences $\Delta t = t_1 - t_2$ in figure 2b has the same temporal pattern as the discharge current shown in figure 2a.

We modeled a higher resolution histogram of the first peak of $h(\Delta t)$ by a convolution of an exponential decay with a time constant τ and a Gaussian distribution with a variance σ . Using the model function

$$h(\Delta t) = \left(\Theta(\Delta t) \cdot e^{-\Delta t/\tau} \right) \otimes \left(e^{-\Delta t^2/(2\sigma^2)} \right) ,$$

where $\Theta(t)$ is a step function, we obtain fit values of $\tau = 2.75 \pm 0.07$ ns and $\sigma = 0.72 \pm 0.03$ ns. The actual shape of this distribution is determined by the discharge network.

Integration over the pair distribution from $t_1 - t_2 = 20$ ns to 62 ns leads to a rate of $n_c = 48.4 \pm 1$ s⁻¹ for photo events of detector D_2 induced by breakdown events of D_1 ; the accidental count rate for that time window,

$$n_{acc} = r_1 r_2 \cdot 42 \text{ ns} = 0.081 \text{ s}^{-1}$$

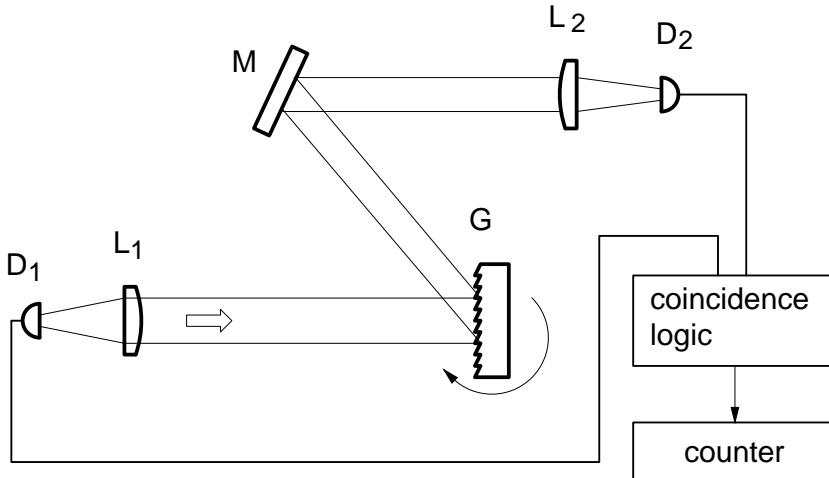


Figure 4: Setup for measuring the breakdown flash spectrum. Light emitted from a diode D_1 is collimated through a lens L_1 with a focal length of $f = 150$ mm, dispersed through a diffraction grating G and detected after a fold mirror M with a second single photon counting APD D_2 after a collimation lens L_2 . The spectrum becomes visible in coincidence events between the two detectors D_1 and D_2 .

is negligible. With the breakdown rate r_1 of D_1 and the captured solid angle Ω_3 , and assuming isotropic emission of the fluorescence light, we obtain a differential breakdown emission intensity of

$$\frac{dn_L}{d\Omega} = \frac{n_c/r_1}{\Omega_3} = 39 \text{ photons/sr}$$

for each detected breakdown of the diode D_1 . From a similar measurement with an aperture diameter of 5 mm, we found a value of $dn_L/d\Omega = 43$ photons/sr. Within the accuracy of the alignment of the photodetectors and the assumption of isotropy of emission, these two values are compatible. However, these values do not contain a detection efficiency η yet. Because this detection efficiency varies with the wavelength (and has a maximum of $\approx 55\%$ at $\lambda \approx 820$ nm[14]), an estimate of total rate can only be given with a knowledge of the spectral distribution.

4 Spectral distribution of the breakdown emission

In order to evaluate possible countermeasures in experiments sensitive to the breakdown light emission of an APD, we measured the spectral distribution of that light. Therefore, we used again a setup of two single photon counting APDs looking at each other, where we inserted a reflection grating as a tunable filter in the optical path as shown in figure 4. The active area of the diode under investigation, D_1 , was placed in the focal plane of a lens L_1 ($f = 150$ mm) to collimate the light emitted in a diode breakdown. The first diffraction order of a blazed grating (1200 lines/mm) was focused with another lens L_2 onto the second APD, D_2 , acting as a photon detector. At a wavelength of 632 nm, we thereby obtain a wavelength resolution of approximately 3.3 nm FWHM; we adjusted the transmitted wavelength by turning the grating.

Again, we identify photons from the breakdown flash in D_1 by looking for coincidences of detector events in D_1 and D_2 . We have chosen a coincidence time window of $\tau_c = 70$ ns after a breakdown of D_1 . In the experiment, we recorded the number of coincidence events, $N_c(\lambda)$, and events $N_1(\lambda), N_2(\lambda)$ of the individual detectors for an integration time T . To obtain acceptable signal levels, we exposed detector D_1 to a raised level of background

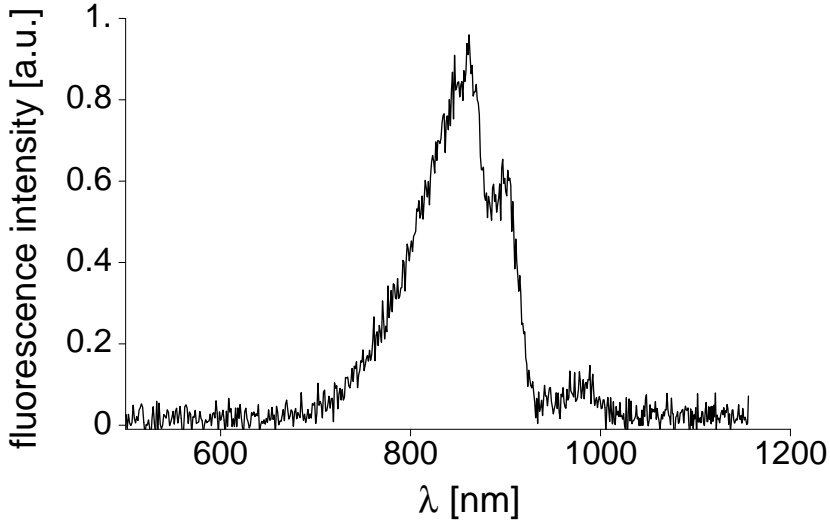


Figure 5: Normalized breakdown flash spectrum of the silicon avalanche photodiode. The emission is peaked around 850 nm. The curve shown is obtained by subtracting the accidental coincidence rate from the raw measured coincidences and subsequent normalization to the count rate of the emitting diode.

light, causing breakdown rates of $N_1/T \approx 17000 \dots 20000 \text{ s}^{-1}$. The corresponding count rate N_2/T of detector D_2 was in the range of $5000 \dots 6000 \text{ s}^{-1}$. The number of coincidence events varied from 300 to 1100 counts over the recording period.

We correct for accidental coincidences and fluctuations in the breakdown rates of APD D_1 , and obtain a normalized spectral distribution $I(\lambda)$ from our experimental data using the expression:

$$I(\lambda) = \alpha \frac{N_c(\lambda) - N_1(\lambda) \cdot N_2(\lambda) \cdot \tau_c/T}{N_1(\lambda)}$$

The spectrum obtained after an integration time of $T = 50$ sec per point is shown in figure 5, using a normalization constant of $\alpha = 10^3$.

One can identify a spectral emission ranging from 700 nm to 1000 nm, with a maximum at 860 nm, two sharp edges at 872 nm and 913 nm, respectively, and two weaker maxima at 900 nm and 980 nm, respectively. This structure is a product of the emission spectrum of the breakdown light, the transfer function of our spectrometer setup and the spectral sensitivity for photo detection of the second avalanche diode D_2 . While the transmission of the spectrometer is reasonably flat over the investigated region, the main deviation between the measured and the emitted spectrum can be attributed to the wavelength dependency of the quantum efficiency $\eta(\lambda)$ of detector D_2 , which, according to the manufacturer, has a smooth drop-off from 70% to 8% in the range of $\lambda = 800$ to 1000 nm[14]. However, the key structures of the spectrum obtained are not an artefact of the detection efficiency, and are characteristic to the generation process of the emitted light.

5 Impact of photoemission on a quantum cryptography system

In our experiments, we tried to quantify the photoemission on breakdown of silicon avalanche photodiodes in Geiger mode. This photoemission may allow a possible eavesdropper in a quantum cryptography application to gain information of the outcome of a measurement

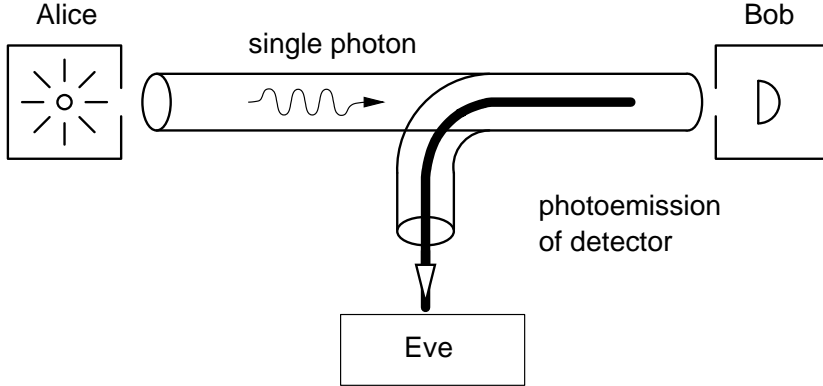


Figure 6: Possible eavesdropping attack to quantum cryptography system. A single photon carrying information on phase or polarization is sent from Alice to Bob without interception by Eve. However, Eve could have access to the photons emitted by Bob upon detection, and gain timing and/or polarization information of the detected photon.

simply by looking at this photoemission, as sketched in figure 6. It therefore has to be ensured that the amount of light leaking back to a possible eavesdropper is small in order to limit its knowledge on the outcome of the single particle measurement by Bob.

To minimize the amount of light generated in the first place, the capacity C_P should be reduced to a minimum. This technique, however, quickly reaches a limit with currently available photodiode packages.

Another measure to reduce the emitted light would be the use of optical filters, blocking the spectral range of 700-1000 nm in which photoemission occurs. However, this technique is restricted to cases where the wavelength of the transmitted light is outside that range. This is the case with recently developed diamond-based single photon sources[9], or using shorter wavelength laser diode emission[15]. For systems using laser diodes around 850 nm exploring an absorption minimum in optical fibers[16], this technique would require narrow band interference filters around the emission wavelength of the diodes. Then, the possible leakage of information to an eavesdropper can be made negligibly small, too.

Additionally, spatial filtering may be used to block light propagating back the quantum channel. Assuming that the photoemission light is emitted without spatial coherence across the photo detection surface, and that light to be detected is coming out of a single spatial mode from an optical fiber or an equivalent spatial mode filter in a free space arrangement, the back-propagating light is reduced.

To estimate the fraction of light coupled back, we first consider the breakdown flash brilliance (i.e., the number of photons emitted per surface area and solid angle) for each photon detection event. From our measurements, we find

$$B = \frac{dn_L}{d\Omega} \cdot \frac{1}{A_D} = 2 \cdot 10^{-3} \frac{\text{photons}}{\text{sr} \cdot \mu\text{m}^2} ,$$

where A_D is the sensitive area of the photodiode. The number of photons N_r collected from such an incoherent source into a single spatial mode, characterized e.g. by a Gaussian beam waist w_0 and a corresponding divergence θ_D , is given by:

$$N_r = B \cdot \int_{r=0}^{\infty} e^{-2r^2/w_0^2} r dr \cdot \int_{2\pi} e^{-2\theta^2/\theta_D^2} d\Omega \approx B \cdot w_0^2 \Theta_D^2 \frac{\pi^2}{4} = B \cdot \frac{\lambda^2}{4}$$

Integrating over a wavelength range from 700 nm to 1050 nm, we obtain a numerical value of $N_r = 3.6 \cdot 10^{-4}$ photons coupled into the single spatial mode of the quantum channel for

a detection event. This value is independent of the detailed structure of the coupling optics as long as reciprocal optical elements are used. It is also only a lower limit obtainable with a similar photodetector, since we have not taken into account the quantum efficiency of the photo detector.

To correct for the quantum efficiency and to estimate the real number of photons coupled back into the quantum channel, we use the measured spectral distribution $I(\lambda)$ and a detection efficiency $\eta(\lambda)$ (i.e., the product of photoelectron generation probability given by the manufacturer and the photoelectron detection efficiency of .55 at 20 V above breakdown) obtained from the manufacturer. Then, we numerically derive a correction factor given by the expression:

$$\beta = \int \frac{I(\lambda)}{\eta(\lambda)} d\lambda \quad / \quad \int I(\lambda) d\lambda$$

For a wavelength range from 700 nm to 1050 nm, we obtain a numerical value of $\beta \approx 3.5$. With this factor, we end up with a corrected numerical value of $N_r^{corr} = \beta N_r = 1.3 \cdot 10^{-3}$ photons coupled back into the single spatial mode of a quantum channel.

6 Summary

To summarize, we quantified the photoemission behavior of a silicon avalanche diode during a breakdown, such as induced by a detection event of a single photon, we found an emission spectrum ranging from 700 nm to 1000 nm, and estimated the possible leak of information to a possible eavesdropper due to this effect. Whereas this emission might have to be considered for single atom and molecule spectroscopy, in quantum cryptography the backdoor for an eavesdropper can be closed by taking some care with spectral and spatial mode filtering. It remains to be investigated if photodiodes used for quantum cryptography systems[17] in the telecom wavelength range (1300 nm and 1550 nm) which are usually based on InGaAs or Ge, show a similar effect. With InGaAs being a direct semiconductor, one could expect it to be more likely for charge carriers to undergo radiative recombinations than in silicon or germanium, thus showing a stronger breakdown flash.

Acknowledgements

This work was supported by the European Union in the EQCSPOT project (EC28139) and the Deutsche Forschungsgemeinschaft.

References

- [1] R. Conradt, 1968, *Z. f. Physik*, **209**, 445.
- [2] W. Haecker, O. Groetzinger, and M.H. Pilkuhn, 1971, *Appl. Phys. Lett.*, **19**, 113.
- [3] H.-K. Lo, S. Popescu, and T. Spiller, 1998, *Introduction to Quantum Computation and Information* (Singapore: World Scientific).
- [4] D. Bouwmeester, A. Ekert, and A. Zeilinger, 2000, *The Physics of Quantum Information* (Berlin: Springer Verlag).
- [5] An updated bibliography on quantum cryptography can be found at <http://www.cs.mcgill.ca/~crepeau/CRYPTO/Biblio-QC.html>
- [6] H. Zbinden, H. Bechman-Pasquinucci, N. Gisin and G. Ribordy, 1998, *Appl. Phys. B*, **67**, 743-748.

- [7] S. Cova, A. Longoni, and A. Andreoni, 1981, *Rev. Sci. Instr.*, **52**(3), 408.
- [8] J.G. Rarity, Private communication.
- [9] C. Kurtsiefer, S. Mayer, P. Zarda, and H. Weinfurter, 2000, *Phys. Rev. Lett.*, **85**, 290.
- [10] W. E. Moerner, and M. Orrit, 1999, *Science*, **283**, 1670-1676
- [11] B. Lounis and W.E. Moerner, 2000, *Nature*, **407**, 491-493.
- [12] R.G.W. Brown, R. Jones, J.G. Rarity and K.D. Ridley, 1987, *Appl. Opt.*, **26**, 2383.
- [13] P. Zarda, 1999, Quantenkryptographie – Ein Experiment im Vergleich. Diploma thesis, University of Innsbruck, Austria.
- [14] Data sheet for the C30902-SDTC diode module, supplied by Perkin-Elmer, formerly EG&G.
- [15] W.T. Buttler, R.J. Hughes, S.K. Lamoreaux, G.L. Morgan, J.E. Nordholt, and C.G. Peterson, 2000, *Phys. Rev. Lett.*, **84**, 5652.
- [16] S. Chingga, P. Zarda, T. Jennewein, and H. Weinfurter, 1999, *Appl. Phys. B*, **69**, 389.
- [17] A. Muller, T. Herzog, B. Huttner, W. Tittel, H. Zbinden and N. Gisin, 1997, *Appl. Phys. Lett.*, **70**, 793-795.